 CMES, vol.16, no.1, pp.57-68, 2006

Meshless Local Petrov-Galerkin Method for Linear Coupled Thermoelastic Analysis

J. Sladek[1], **V. Sladek**[1], **Ch. Zhang**[2], **C.L. Tan**[3]

Abstract: The Meshless Local Petrov-Galerkin (MLPG) method for linear transient coupled thermoelastic analysis is presented. Orthotropic material properties are considered here. A Heaviside step function as the test functions is applied in the weak-form to derive local integral equations for solving two-dimensional (2-D) problems. In transient coupled thermoelasticity an inertial term appears in the equations of motion. The second governing equation derived from the energy balance in coupled thermoelasticity has a diffusive character. To eliminate the time-dependence in these equations, the Laplace-transform technique is applied to both of them. Local integral equations are written on small sub-domains with a circular shape. They surround nodal points which are distributed over the analyzed domain. The spatial variation of the displacements and temperature are approximated by the Moving Least-Squares (MLS) scheme. After performing the spatial integrations, a system of linear algebraic equations for unknown nodal values is obtained. The boundary conditions on the global boundary are satisfied by the collocation of the MLS-approximation expressions for the displacements and temperature at the boundary nodal points. The Stehfest's inversion method is then applied to obtain the final time-dependent solutions.

keyword: Transient coupled thermoelasticity, Orthotropic materials, Moving least-squares interpolation, 2-D problems, Laplace-transform, Stehfest's inversion

1 Indroduction

Dynamic thermoelasticity is relevant for many engineering problems since thermal stresses play an important role in the integrity of structures. In the case of traditional materials thermal effects on a body are limited to strains due to the temperature gradient. For sophisticated materials such as high performance composites thermal effects can include heat production due to the strain rate, i.e. the thermoelastic dissipation. Several computational methods have been proposed over the past years to analyze thermoelasticity problems. Many of them have been directed to uncoupled problems in steady or transient heat conduction states. Few investigations have been done successfully for coupled thermoelasticity. Domain-based approaches, particularly those involving the finite element method (FEM), have been developed and applied to thermoelasticity [Keramidas and Ting (1976); Prevost and Tao (1983); Cannarozzi and Ubertini (2001)]. The boundary element method (BEM), recognized since many years as a powerful tool in numerical analysis, was applied for the first time to transient uncoupled thermoelasticity by Rizzo and Shippy (1977). Shiah and Tan (1999) applied the BEM for 2-D uncoupled thermoelasticity in anisotropic solids. Thermomechanical crack growth has been investigated by Prasad (1998) using a dual BEM. Particular integral formulations for 2-D and 3-D transient uncoupled thermoelastic analyses have been presented by Park and Banerjee (2002). The BEM has been successfully applied also to coupled thermoelastic problems [Sladek and Sladek (1984); Dargush and Banerjee (1991); Chen and Dargush (1995); Suh and Tosaka (1989); Hosseini-Tehrani and Eslami (2000)]. Dual reciprocity BEM has been presented by Gaul *et al*. (2003), and Kögl and Gaul (2000, 2003).

Recently developed sophisticated materials with thermoelastic dissipation are composites with anisotropic properties. Governing equations for coupled thermal and mechanical fields with anisotropic material properties are much more complex than those in uncoupled thermoelasticity for isotropic materials. Thus, efficient computational methods are required to solve the boundary or the initial-boundary value thermoelastic problems for

[1] Institute of Construction and Architecture, Slovak Academy of Sciences, 84503 Bratislava, Slovakia
[2] Department of Civil Engineering, University of Siegen, D-57068 Siegen, Germany
[3] Department of Mechanical & Aerospace Engineering, Carleton University, Ottawa, Canada

anisotropic solids. In recent years, an increasing attention has been paid to the numerical analysis of coupled thermoelasticity problems. In spite of the great success of the FEM and BEM as effective numerical tools for the solution of boundary or initial-boundary value problems in elasticity, there is still a growing interest in the development of new advanced methods. In particular, meshless formulations are becoming popular due to their high adaptivity and low costs to prepare input and output data for numerical analyses. A variety of meshless methods has been proposed so far and some of them also applied to transient heat conduction problems [Batra et al. (2003); Sladek et al. (2003a,b, 2004a, 2006); Qian and Batra (2004); Wang et al. (2006)] or to thermoelastic problems [Sladek et al. (2001); Bobaru and Mukherjee (2003); Qian and Batra (2004)].

The meshless method can be obtained from a weak-form formulation on either the global domain or a set of local subdomains. In the global formulation background cells are required for the integration of the weak-form. In methods based on local weak-form formulation, no background cells are required and therefore they are often referred to as truly meshless methods. The meshless local Petrov-Galerkin (MLPG) method is a fundamental base for the derivation of many meshless formulations, since trial and test functions can be chosen from different functional spaces. By using the fundamental solution as the test function, accurate numerical results can be obtained, which were reported in previous papers for 2-D transient heat conduction problems in isotropic, homogeneous or continuously nonhomogeneous solids [Sladek et al. (2003a,b)], elasticity under static and dynamic loads [Atluri et al. (2000, 2003); Sellountos and Polyzos (2003); Sellountos et al. (2005)], and for 3-D problems in homogeneous and isotropic solids under a static or a dynamic load [Han and Atluri (2004a,b)].

In this paper, the MLPG method with a Heaviside step function as the test functions [Atluri et al. (2003); Atluri (2004); Sladek et al. (2004a,b)] is applied to solve two-dimensional transient coupled thermoelasticity problems. An inertial term exists in the equations of motion for transient thermoelasticity. The second governing equation derived from the energy balance has a diffusive character. To eliminate the time-dependences in both governing partial differential equations, the Laplace-transform technique is applied such that they are satisfied in the Laplace-transformed domain in a weak-form on small fictitious subdomains. If the shape of subdomains has a simple form, numerical integrations over them can be easily carried out. Nodal points are introduced and distributed over the analyzed domain and each of them is surrounded by a small circle for simplicity, but without loss of generality. The integral equations have a very simple nonsingular form. The spatial variations of the displacements and temperature are approximated by the Moving Least-Squares (MLS) scheme [Belytschko et al. (1996); Zhu et al. (1998)]. After performing the spatial integrations, a system of linear algebraic equations for unknown nodal values is obtained. The boundary conditions on the global boundary are satisfied by the collocation of the MLS-approximation expressions for the displacements and temperature at the boundary nodal points. To obtain the final time-dependent solutions, the Stehfest's inversion method [Stehfest (1970)] is applied. The accuracy and the efficiency of the proposed MLPG method are verified by numerical examples.

2 The MLPG in transient coupled thermoelasticity

A homogeneous, orthotropic and linear elastic solid is considered. The equilibrium and the thermal balance equations in transient coupled thermoelasticity [Nowacki (1986)] can be written as

$$\sigma_{ij,j}(\mathbf{x},\tau) - \rho\ddot{u}_i(\mathbf{x},\tau) + X_i(\mathbf{x},\tau) = 0, \tag{1}$$

$$[k_{ij}(\mathbf{x})\theta_{,j}(\mathbf{x},\tau)]_{,i} - \rho c\dot{\theta}(\mathbf{x},\tau) - \gamma_{ij}\theta_0\dot{u}_{i,j}(\mathbf{x},\tau) + Q(\mathbf{x},\tau) = 0, \tag{2}$$

where σ_{ij}, τ, θ, θ_0, u_i, X_i and Q are the stress, time, temperature difference, reference temperature, displacement, density of body force vector and density of heat sources, respectively. Also, ρ, k_{ij}, c and γ_{ij} and are the mass density, thermal conductivity tensor, specific heat, stress-temperature modulus, respectively. The dots over a quantity indicate the time derivatives. A static problem can be considered formally as a special case of the dynamic one, by omitting the acceleration $\ddot{u}_i(\mathbf{x},\tau)$ in the equations of motion (1) and the time derivative terms in equation (2). Therefore, both cases are analyzed in this paper.

In the case of orthotropic materials, the relation between the stress σ_{ij} and the strain ε_{ij} when temperature changes are considered, is governed by the well known Duhamel-Neumann constitutive equations for the stress tensor

$$\sigma_{ij}(\mathbf{x},\tau) = c_{ijkl}\varepsilon_{kl}(\mathbf{x},\tau) - \gamma_{ij}\theta(\mathbf{x},\tau), \tag{3}$$

where c_{ijkl} are the material stiffness coefficients. The stress-temperature modulus can be expressed through the stiffness coefficients and the coefficients of linear thermal expansion α_{kl}

$$\gamma_{ij} = c_{ijkl}\alpha_{kl}\,. \tag{4}$$

For plane problems the constitutive equation (3) is frequently written in terms of the second-order tensor of elastic constants [Lekhnitskii (1963)]. The constitutive equation for orthotropic materials and plane strain problems has the following form

$$\begin{aligned}\begin{bmatrix}\sigma_{11}\\ \sigma_{22}\\ \sigma_{12}\end{bmatrix} &= \begin{bmatrix} c_{11} & c_{12} & 0\\ c_{12} & c_{22} & 0\\ 0 & 0 & c_{66}\end{bmatrix}\begin{bmatrix}\varepsilon_{11}\\ \varepsilon_{22}\\ 2\varepsilon_{12}\end{bmatrix}\\ &- \begin{bmatrix} c_{11} & c_{12} & c_{13}\\ c_{12} & c_{22} & c_{23}\\ 0 & 0 & 0\end{bmatrix}\begin{bmatrix}\alpha_{11}\\ \alpha_{22}\\ \alpha_{33}\end{bmatrix}\theta\\ &= \mathbf{C}\begin{bmatrix}\varepsilon_{11}\\ \varepsilon_{22}\\ 2\varepsilon_{12}\end{bmatrix} - \gamma\theta,\end{aligned} \tag{5}$$

$$\text{with } \gamma = \begin{bmatrix} c_{11} & c_{12} & c_{13}\\ c_{12} & c_{22} & c_{23}\\ 0 & 0 & 0\end{bmatrix}\begin{bmatrix}\alpha_{11}\\ \alpha_{22}\\ \alpha_{33}\end{bmatrix} = \begin{bmatrix}\gamma_{11}\\ \gamma_{22}\\ 0\end{bmatrix}.$$

Equation (5) can be reduced to a simple form for isotropic materials

$$\sigma_{ij} = 2\mu\varepsilon_{ij} + \lambda\varepsilon_{kk}\delta_{ij} - (3\lambda+2\mu)\alpha\theta\delta_{ij} \quad , \tag{6}$$

with Lame's constants λ and μ.

The following essential and natural boundary conditions are assumed for the mechanical quantities

$u_i(\mathbf{x},\tau) = \tilde{u}_i(\mathbf{x},\tau)$ on Γ_u,

$t_i(\mathbf{x},\tau) = \sigma_{ij}(\mathbf{x},\tau)n_j(\mathbf{x}) = \tilde{t}_i(\mathbf{x},\tau)$ on Γ_t,

and for the thermal quantities

$\theta(\mathbf{x},\tau) = \tilde{\theta}(\mathbf{x},\tau)$ on Γ_p,

$q(\mathbf{x},\tau) = k_{ij}\theta_{,j}(\mathbf{x},\tau)n_i(\mathbf{x}) = \tilde{q}(\mathbf{x},\tau)$ on Γ_q,

where Γ_u is the part of the global boundary with prescribed displacements, while on Γ_t, Γ_p and Γ_q the traction vector t_i, temperature and the heat flux q are prescribed, respectively.

Initial conditions for the mechanical and thermal quantities have to be prescribed

$u_i(\mathbf{x},\tau)|_{\tau=0} = u_i(x,0)$ and $\dot{u}_i(\mathbf{x},\tau)|_{\tau=0} = \dot{u}_i(x,0)$

$\theta(\mathbf{x},\tau)|_{\tau=0} = \theta(x,0)$ in Ω.

Applying the Laplace-transform to the governing equations (1) and (2) we obtain

$$\overline{\sigma}_{ij,j}(\mathbf{x},p) - \rho p^2\overline{u}_i(\mathbf{x},p) = -\overline{F}_i(\mathbf{x},p), \tag{7}$$

$$\begin{aligned}&\left[k_{ij}(\mathbf{x})\overline{\theta}_{,j}(\mathbf{x},p)\right]_{,i} - \rho c p\overline{\theta}(\mathbf{x},p)\\ &\quad - \gamma_{ij}\theta_0 p\overline{u}_{i,j}(\mathbf{x},p) + \overline{R}(\mathbf{x},p) = 0,\end{aligned} \tag{8}$$

where

$$\overline{F}_i(\mathbf{x},p) = \overline{X}_i(\mathbf{x},p) + pu_i(\mathbf{x},0) + \dot{u}_i(\mathbf{x},0),$$

$$\overline{R}(\mathbf{x},p) = \overline{Q}(\mathbf{x},p) + \theta(\mathbf{x},0)$$

are the re-defined body forces and heat source, respectively, in the Laplace-transformed domain with the initial boundary conditions for the displacements $u_i(\mathbf{x},0)$, velocities $\dot{u}_i(\mathbf{x},0)$ and temperature $\theta(\mathbf{x},0)$.

The Laplace-transform of a function $f(\mathbf{x},\tau)$ is defined as

$$L[f(x,\tau)] = \overline{f}(x,p) = \int_0^\infty f(x,\tau)e^{-p\tau}d\tau,$$

where p is the Laplace-transform parameter.

Instead of writing the global weak-form for the above governing equations, the MLPG method constructs a weak-form over the local fictitious subdomains such as Ω_s, which is a small region taken for each node inside the global domain [Atluri (2004)]. The local subdomains overlap each other, and cover the whole global domain Ω. The local subdomains could be of any geometrical shape and size. In the present paper, the local subdomains are taken to be of circular shape. The local weak-form of the governing equations (7) can be written as

$$\int_{\Omega_s}\left[\overline{\sigma}_{ij,j}(\mathbf{x},p) - \rho p^2\overline{u}_i(\mathbf{x},p) + \overline{F}_i(\mathbf{x},p)\right]\, u^*_{ik}(\mathbf{x})\, d\Omega = 0, \tag{9}$$

where $u^*_{ik}(\mathbf{x})$ is a test function.

Using

$$\overline{\sigma}_{ij,j}u^*_{ik} = \left(\overline{\sigma}_{ij}u^*_{ik}\right)_{,j} - \overline{\sigma}_{ij}u^*_{ik,j}$$

and applying the Gauss divergence theorem one can write

$$\int_{\partial\Omega_s} \overline{\sigma}_{ij}(\mathbf{x},p)n_j(\mathbf{x})u^*_{ik}(\mathbf{x})d\Gamma - \int_{\Omega_s} \overline{\sigma}_{ij}(\mathbf{x},p)u^*_{ik,j}(\mathbf{x})d\Omega + \int_{\Omega_s} \left[-\rho p^2 \overline{u}_i(\mathbf{x},p) + \overline{F}_i(\mathbf{x},p)\right] u^*_{ik}(\mathbf{x})d\Omega = 0, \quad (10)$$

where $\partial\Omega_s$ is the boundary of the local subdomain which consists of three parts $\partial\Omega_s = L_s \cup \Gamma_{st} \cup \Gamma_{su}$ [Atluri (2004)]. Here, L_s is the local boundary that is totally inside the global domain, Γ_{st} is the part of the local boundary which coincides with the global traction boundary, i.e., $\Gamma_{st} = \partial\Omega_s \cap \Gamma_t$, and similarly Γ_{su} is the part of the local boundary that coincides with the global displacement boundary, i.e., $\Gamma_{su} = \partial\Omega_s \cap \Gamma_u$.

By choosing a Heaviside step function as the test function $u^*_{ik}(\mathbf{x})$ in each subdomain

$$u^*_{ik}(\mathbf{x}) = \begin{cases} \delta_{ik} & \text{at } \mathbf{x} \in \Omega_s \\ 0 & \text{at } \mathbf{x} \notin \Omega_s \end{cases}$$

and considering

$$\overline{t}_i(\mathbf{x},p) = \overline{\sigma}_{ij}(\mathbf{x},p)n_j(\mathbf{x}),$$

the local weak-form (10) is converted to the following local boundary-domain integral equations

$$\int_{\partial\Omega_s} \overline{t}_i(\mathbf{x},p)d\Gamma + \int_{\Omega_s} \left[-\rho p^2 \overline{u}_i(\mathbf{x},p) + \overline{F}_i(\mathbf{x},p)\right] d\Omega = 0. \quad (11)$$

Rearranging the unknown terms on the left hand side we get

$$\int_{L_s+\Gamma_{su}} \overline{t}_i(\mathbf{x},p)d\Gamma - \int_{\Omega_s} \rho p^2 \overline{u}_i(\mathbf{x},p)d\Omega = -\int_{\Gamma_{st}} \tilde{\overline{t}}_i(\mathbf{x},p)d\Gamma - \int_{\Omega_s} \overline{F}_i(\mathbf{x},p)d\Omega. \quad (12)$$

Equation (12) represents overall force equilibrium on the subdomain Ω_s in the D'Lambert sense. In the case of stationary problems the domain integral on the left-hand side of the local boundary-domain integral equations disappears. A pure boundary integral formulation is then obtained under the assumption of vanishing body forces and homogeneous initial conditions.

Similarly, the local weak-form of the governing equation (8) can be written as

$$\int_{\Omega_s} \Big\{ \left[k_{ij}(\mathbf{x})\overline{\theta}_{,j}(\mathbf{x},p)\right]_{,i} - \rho c p \overline{\theta}(\mathbf{x},p) - \gamma_{ij}\theta_0 p \overline{u}_{i,j}(\mathbf{x},p) + \overline{R}(\mathbf{x},p)\Big\} u^*(\mathbf{x})\, d\Omega = 0, \quad (13)$$

where $u^*(\mathbf{x})$ is a test function.

Applying the Gauss divergence theorem to the local weak-form and considering the Heaviside step function for the test function $u^*(\mathbf{x})$ one can obtain

$$\int_{L_s+\Gamma_{sp}} \overline{q}(\mathbf{x},p)d\Gamma - \int_{\Omega_s} \rho c p \overline{\theta}(x,p)d\Omega - \int_{\Omega_s} \gamma_{ij}\theta_0 p \overline{u}_{i,j}(\mathbf{x},p)d\Omega = -\int_{\Gamma_{sq}} \tilde{\overline{q}}(\mathbf{x},p)d\Gamma - \int_{\Omega_s} \overline{R}(\mathbf{x},p)d\Omega. \quad (14)$$

Equation (14) is similarly recognized as the energy balance condition on the subdomain.

3 Numerical solution

In the MLPG method the test and the trial functions are not necessarily from the same functional spaces. For internal nodes, the test functions are chosen as the Heaviside step function with its support on the local subdomain. The trial functions, on the other hand, are chosen to be the moving least-squares (MLS) approximation over a number of nodes which are spread within the domain of influence. The approximated functions for the Laplace-transforms of the displacements and the temperature can be written as [Atluri (2004)]

$$\overline{\mathbf{u}}^h(\mathbf{x},p) = \mathbf{\Phi}^T(\mathbf{x}) \cdot \hat{\mathbf{u}}(p) = \sum_{a=1}^{n} \phi^a(\mathbf{x})\hat{\mathbf{u}}^a(p),$$

$$\overline{\theta}^h(\mathbf{x},p) = \sum_{a=1}^{n} \phi^a(\mathbf{x})\hat{\theta}^a(p), \quad (15)$$

where the nodal values $\hat{\mathbf{u}}^a(p)$ and $\hat{\theta}^a(p)$ are fictitious parameters for the displacements and the temperature, respectively and $\phi^a(\mathbf{x})$ is the shape function associated with the node a. The number of nodes n used for the approximation is determined by the weight function $w^a(\mathbf{x})$. In literature Gaussian distribution function or splines are usually used as the weight function [Atluri (2004)]. Gaussian distribution function has only C^0-continuity and it

is not convenient for modeling the gradients of displacements and temperature. Therefore, a 4^{th} order spline type weight function is applied in the present work

$$w^a(\mathbf{x}) = \begin{cases} 1-6\left(\frac{d^a}{r^a}\right)^2+8\left(\frac{d^a}{r^a}\right)^3-3\left(\frac{d^a}{r^a}\right)^4, & 0 \le d^a \le r^a \\ 0, & d^a \ge r^a \end{cases} \tag{16}$$

where $d^a = \|\mathbf{x}-\mathbf{x}^a\|$ and r^a is the size of the support domain. It is seen that the C^1-continuity is ensured over the entire domain, therefore the continuity conditions of the tractions and the heat flux are satisfied. Splines of 7^{th} order with C^3-continuity are used for problems with higher order derivatives in local integral equations and it is not required to apply them in our case.

The traction vectors $\overline{t}_i(\mathbf{x},p)$ at a boundary point $\mathbf{x} \in \partial\Omega_s$ are approximated in terms of the same nodal values $\hat{\mathbf{u}}^a(p)$ as

$$\overline{\mathbf{t}}^h(\mathbf{x},p) = \mathbf{N}(\mathbf{x})\mathbf{C}\sum_{a=1}^{n}\mathbf{B}^a(\mathbf{x})\hat{\mathbf{u}}^a(p) - \mathbf{N}(\mathbf{x})\gamma\sum_{a=1}^{n}\phi^a(\mathbf{x})\hat{\theta}^a(p), \tag{17}$$

where the matrix $\mathbf{N(x)}$ is related to the normal vector $\mathbf{n(x)}$ on $\partial\Omega_s$ by

$$\mathbf{N}(\mathbf{x}) = \begin{bmatrix} n_1 & 0 & n_2 \\ 0 & n_2 & n_1 \end{bmatrix},$$

and the matrix $\mathbf{B}^a$ is represented by the gradients of the shape functions as

$$\mathbf{B}^a = \begin{bmatrix} \phi^a_{,1} & 0 \\ 0 & \phi^a_{,2} \\ \phi^a_{,2} & \phi^a_{,1} \end{bmatrix}.$$

Similarly the heat flux $\overline{q}(\mathbf{x},p)$ can be approximated by

$$\overline{q}^h(\mathbf{x},p) = k_{ij}n_i\sum_{a=1}^{n}\phi^a_{,j}(\mathbf{x})\hat{\theta}^a(p). \tag{18}$$

Satisfying the boundary conditions at those nodal points on the global boundary, where the displacements and the temperature are prescribed, and making use of the approximation formula (15), one may write the discretized forms of the boundary conditions as

$$\sum_{a=1}^{n}\phi^a(\zeta)\hat{\mathbf{u}}^a(p) = \tilde{\overline{\mathbf{u}}}(\zeta,p) \text{ for } \zeta \in \Gamma_u, \tag{19}$$

$$\sum_{a=1}^{n}\phi^a(\zeta)\hat{\theta}^a(p) = \tilde{\overline{\theta}}(\zeta,p) \text{ for } \zeta \in \Gamma_p. \tag{20}$$

Furthermore, from the MLS-approximations, equations (17) and (18), for the unknown quantities in the local boundary-domain integral equations (12) and (14), their discretized forms are

$$\begin{aligned} &\sum_{a=1}^{n}\left(\int_{L_s+\Gamma_{su}}\mathbf{N}(\mathbf{x})\mathbf{C}\mathbf{B}^a(\mathbf{x})d\Gamma - \mathbf{I}\rho p^2\int_{\Omega_s}\phi^a(\mathbf{x})d\Omega\right)\hat{\mathbf{u}}^a(p) \\ &\quad -\sum_{a=1}^{n}\left(\int_{L_s+\Gamma_{su}}\mathbf{N}(\mathbf{x})\gamma\phi^a(\mathbf{x})d\Gamma\right)\hat{\theta}^a(p) \\ &\quad = -\int_{\Gamma_{st}}\tilde{\overline{\mathbf{t}}}(\mathbf{x},p)d\Gamma - \int_{\Omega_s}\overline{\mathbf{F}}(\mathbf{x},p)d\Omega, \end{aligned} \tag{21}$$

$$\begin{aligned} &\sum_{a=1}^{n}\left(\int_{L_s+\Gamma_{sp}}\mathbf{n}^T\mathbf{K}\mathbf{P}^a(\mathbf{x})d\Gamma - \int_{\Omega_s}\rho c p\phi^a(\mathbf{x})d\Gamma\right)\hat{\theta}^a(p) \\ &\quad -\sum_{a=1}^{n}\left(\int_{\Omega_s}\theta_0 p\gamma^T\mathbf{B}^a(\mathbf{x})d\Gamma\right)\hat{\mathbf{u}}^a(p) \\ &\quad = -\int_{\Gamma_{sq}}\tilde{\overline{q}}(\mathbf{x},p)d\Gamma - \int_{\Omega_s}\overline{R}(\mathbf{x},p)d\Omega, \end{aligned} \tag{22}$$

which are considered on the sub-domains adjacent to interior nodes as well as to the boundary nodes on Γ_{st} and Γ_{sq}. In equation (21), $\mathbf{I}$is a unit matrix defined by

$$\mathbf{I} = \begin{pmatrix} 1 & 0 \\ 0 & 1 \end{pmatrix}$$

and in equation (22), we have used the notations

$$\mathbf{G} = \begin{bmatrix} \gamma_{11} & \gamma_{12} \\ \gamma_{12} & \gamma_{22} \end{bmatrix}, \quad \mathbf{K} = \begin{bmatrix} k_{11} & k_{12} \\ k_{12} & k_{22} \end{bmatrix},$$

$$\mathbf{P}^a(\mathbf{x}) = \begin{bmatrix} \phi^a_{,1} \\ \phi^a_{,2} \end{bmatrix}, \quad \mathbf{n}^T = (n_1, n_2).$$

Collecting the discretized local boundary-domain integral equations together with the discretized boundary conditions for the displacements and the temperature results in the complete system of linear algebraic equations for the computation of the nodal unknowns, namely, the Laplace-transforms of the fictitious parameters $\hat{\mathbf{u}}^a(p)$

and $\hat{\theta}^a(p)$. The time dependent values of the transformed quantities can be obtained by an inverse Laplace-transform. In the present analysis, the Stehfest's inversion algorithm [Stehfest (1970)] is used.

4 Numerical examples

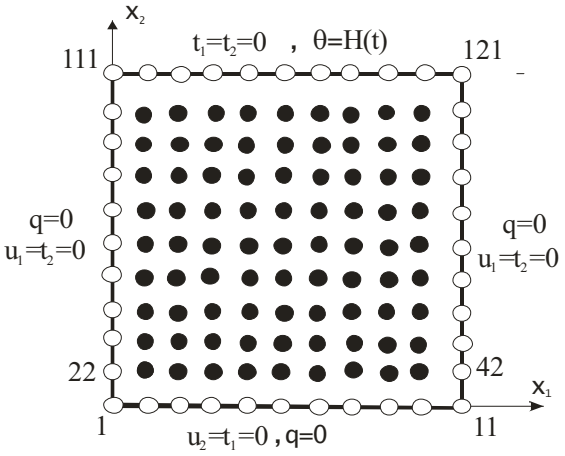

Figure 1 : A suddenly heated unit square panel

In order to test the accuracy of the present meshless method a unit square panel under a sudden heating on the top side is analyzed as the first example (Fig. 1). The following analytical solution is available for uncoupled thermoelasticity in an isotropic material [Carslaw and Jaeger (1959)]

$$\theta(x_2,\tau) = 1 - \frac{4}{\pi}\sum_{n=0}^{\infty}\frac{(-1)^n}{2n+1}\exp\left[-\frac{(2n+1)^2\pi^2\kappa\tau}{4a^2}\right]\times \cos\left(\frac{(2n+1)\pi x_2}{2a}\right),$$

$$u_2(x_2,\tau) = \frac{(1+\nu)\alpha}{(1-\nu)}\int_0^{x_2}\theta(x_2,\tau)dx_2,$$

$$\sigma_{11}(x_2,\tau) = -\frac{\alpha E}{(1-\nu)}\theta(x_2,\tau), \tag{23}$$

where a is the side length of the panel and $\kappa = k/\rho c$ is the diffusivity coefficient. In the numerical analysis here, the following material constants are used: $k = 1$, $\rho = 1$, $c = 1$, thermal expansion coefficient $\alpha = 0.02$, Young's modulus $E = 1$ and Poisson's ratio $\nu = 0.3$. Also, plane strain condition is assumed.

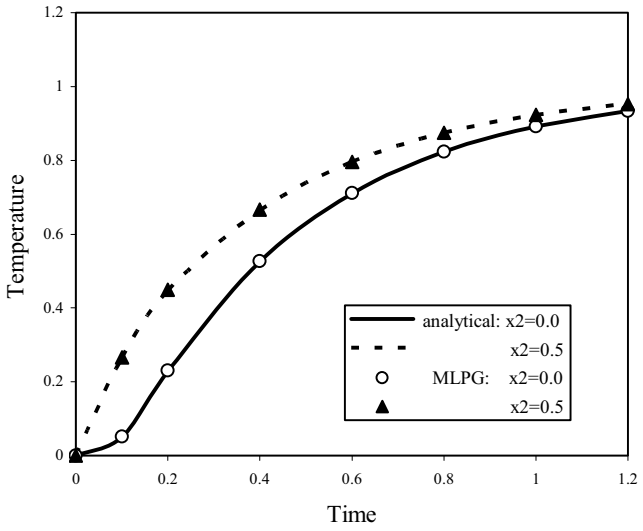

Figure 2 : Temporal variation of the temperature at two different points on x_2- axis

The mechanical displacement and the thermal fields on the finite square panel are approximated by using 121 (11x11) equi-spaced nodes. The local sub-domains are considered to be circular, each with a radius $r_{loc} = 0.08$.

It can be seen from Fig. 2 that there is an excellent agreement of the present results with the exact solution for the time variation of the temperature at the two points considered. For the purpose of error analysis the Sobolev-norm is calculated. The relative error of the temperature in the considered time interval $[0,T]$ is defined as

$$r = \frac{\|\theta^{num} - \theta^{exact}\|}{\|\theta^{exact}\|}, \tag{24}$$

where $T = 1.2$ and

$$\|\theta\| = \left(\int_0^T \theta^2 d\tau\right)^{1/2}.$$

The relative error of the temperature, r, at both points is less than 0.5%. For the total number of 441 nodes, the relative error $r = 0.15\%$ has been obtained.

Numerical results for the displacement u_2 at the free-end of the panel and at the mid-point of the x_2- axis are presented in Fig. 3. They are compared again with the analytical results and an excellent agreement is observed too. Numerical results for the direct stress σ_{11} are presented in Fig. 4, where it can be seen again that there

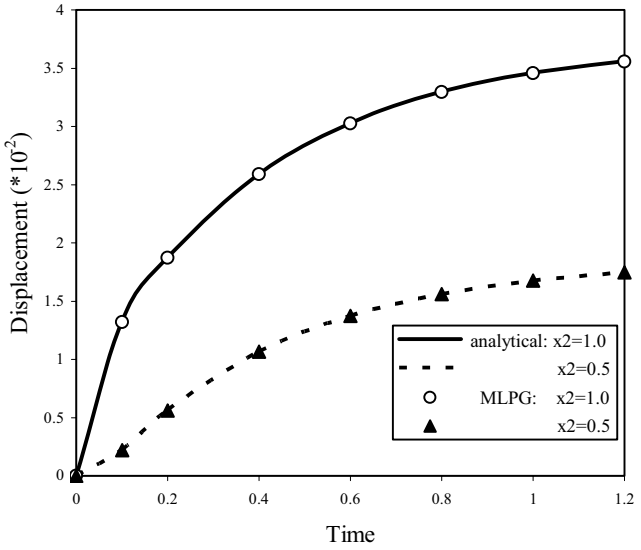

Figure 3 : Temporal variation of the displacement u_2 at two different points on x_2- axis

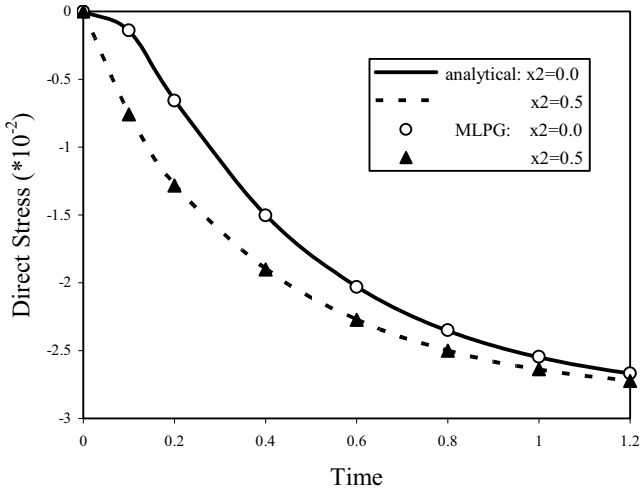

Figure 4 : Temporal variation of the stress σ_{11}

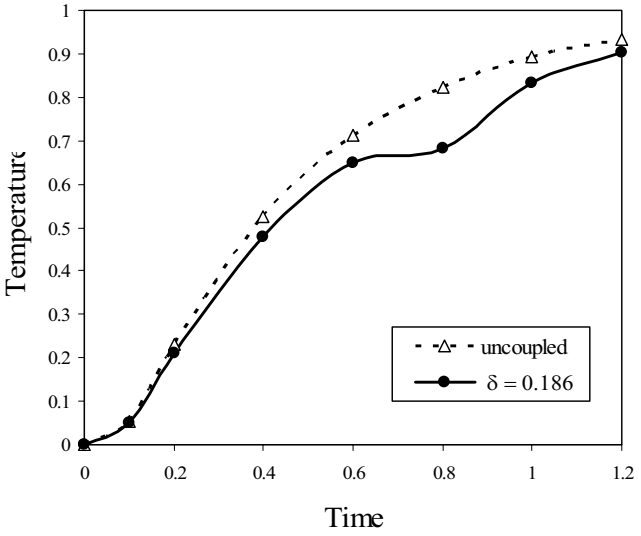

Figure 5 : Coupling effect on the temporal variation of the temperature at $x_2 = 0$

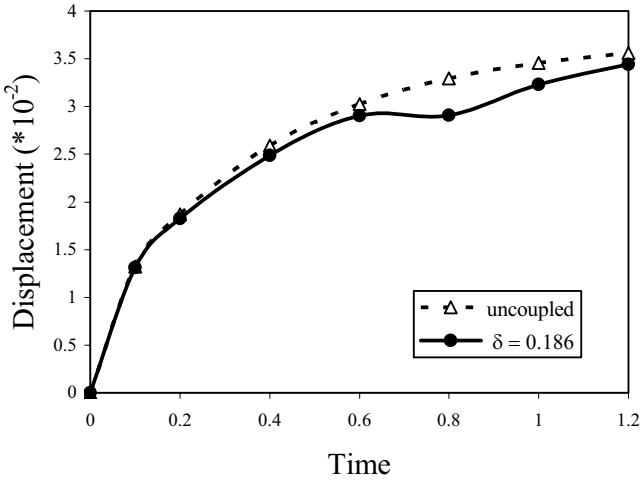

Figure 6 : Coupling effect on the temporal variation of the displacement u_2 at $x_2 = 1$

is an excellent agreement of the present results and the exact solution at both points considered.

Next, the coupling effect is analyzed in the same sample. A measure of the thermoelastic coupling is given by the dimensionless thermoelastic coupling parameter [Cannarozzi and Ubertini (2001)]

$$\delta = \frac{(1+\nu)\alpha^2 E\theta_0}{(1-\nu)(1-2\nu)\rho c},$$

where $\delta = 0$ corresponds to the uncoupled case. For traditional materials, δ ranges from 0.01 to 0.1. Here, the thermoelastic coupling parameter is $\delta = 0.186$, which corresponds to $\theta_0 = 100$ and the previously used material constants. The coupling effects on the temperature and the displacement u_2 at points $x_2 = 0$ and $x_2 = 1$, respectively, are presented in Figs. 5 and 6. One can observe that the influence of the mechanical-thermal coupling on both quantities is weaker for small and large time instants. The strongest influence appears at about $\tau = 0.8$ for the considered material constants. A similar phenomenon has been observed also for a suddenly heated half-space analyzed by Chen and Dargush (1995),

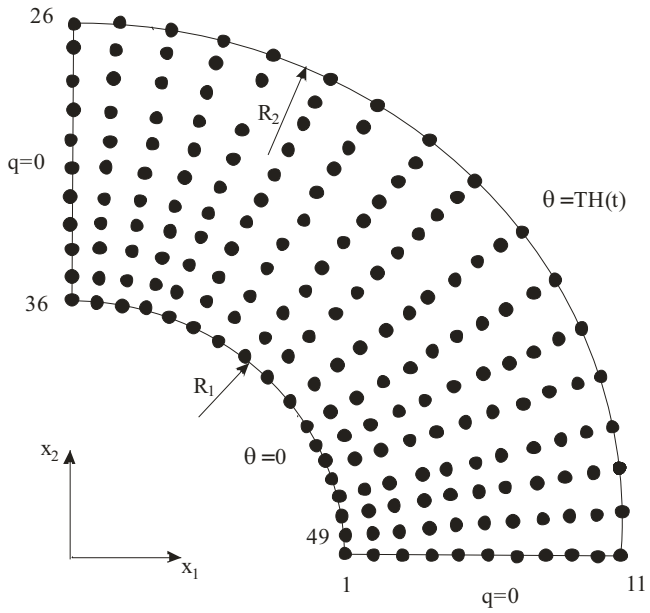

Figure 7 : A suddenly heated hollow cylinder

and Hosseini-Tehrani and Eslami (2000).

In the second numerical example a hollow cylinder with a prescribed Heaviside time variation of the temperature on the outer surface is analyzed. On the inner surface with radius $R_1 = 8$ the temperature is kept at zero value. The ratio of the outer and the inner radii is considered as $R_2/R_1 = 2$. The following material constants for an isotropic hollow cylinder are considered: $k = 1$, $\rho = 1$, $c = 1$, $\alpha = 0.02$, $E = 1$ and $\nu = 0.25$. For the numerical calculations, 176 nodes with a regular node distribution in the radial direction are employed, see Fig. 7. The local sub-domains are considered to be circular with a radius $r_{loc} = 0.6$.

In the uncoupled theory, the exact solutions for the temperature, the radial displacement and the hoop stresses for this problem can be obtained as [Carslaw and Jaeger (1959), Timoshenko and Goodier (1951)]

$$\theta(r,\tau) = T\frac{\ln(r/R_1)}{\ln(R_2/R_1)} - \pi\sum_{n=1}^{\infty} T\frac{J_0^2(R_1\alpha_n)U_0(r\alpha_n)}{J_0^2(R_1\alpha_n) - J_0^2(R_2\alpha_n)}\exp(-\kappa\alpha_n^2\tau),$$

$$u_r(r,\tau) = \frac{(1+\nu)\alpha}{(1-\nu)}\frac{1}{r}\int_{R_1}^{r}\theta(x,\tau)xdx + C_1 r + \frac{C_2}{r},$$

$$\sigma_{\varphi\varphi} = \frac{\alpha E}{1-\nu}\frac{1}{r^2}\int_{R_1}^{r}\theta(x,\tau)xdx - \frac{\alpha E}{1-\nu}\theta(r,\tau) + \frac{E}{1-\nu}\left(\frac{C_1}{1-2\nu} + \frac{C_2}{r^2}\right), \quad (25)$$

where

$$U_0(r\alpha_n) = J_0(r\alpha_n)Y_0(\alpha_n R_2) - J_0(\alpha_n R_2)Y_0(r\alpha_n),$$

and α_n are the roots of the following transcendental equation

$$J_0(r)Y_0(rR_2/R_1) - J_0(rR_2/R_1)Y_0(r) = 0,$$

with $J_0(r)$ and $Y_0(r)$ being the Bessel functions of the first and the second kind and zero-th order. The constants C_1 and C_2 in equation (25) are defined as

$$C_1 = \frac{(1-2\nu)\alpha(1+\nu)}{1-\nu}\frac{1}{R_2^2 - R_1^2}\int_{R_1}^{R_2}\theta(r,\tau)rdr,$$

$$C_2 = \frac{\alpha(1+\nu)}{1-\nu}\frac{R_1^2}{R_2^2 - R_1^2}\int_{R_1}^{R_2}\theta(r,\tau)rdr \quad .$$

The computed results of the time variations of the temperature at the mid-radius $r = 12$ for uncoupled and coupled problems are shown in Fig. 8. For the uncoupled problem, the numerical results are compared with the exact solution (25) and an excellent agreement is obtained. For the coupled case, θ_0 is selected as 150 for the purpose of illustration. With $\theta_0 = 150$, for which $\delta = 0.2$, it is evident that the temperature is lower in the entire time interval in the coupled case as compared to the uncoupled one.

The temporal variations of the hoop stress at the inner surface are presented in Fig. 9. Here, relatively lower values of the hoop stress are obtained in the coupled problem; this is due to the lower temperature distribution. The corresponding variations of the hoop stress at the outer surface are shown in Fig. 10. The influence of the mechanical-thermal coupling on the hoop stress is similar at both surfaces. The radial displacement is computed at the mid-radius of the hollow cylinder. The numerical results for both coupled and uncoupled cases are presented in Fig. 11.

In the third numerical example, an orthotropic square panel is analyzed. The boundary conditions are the same as those in the first example, see Fig.1. A unit side length

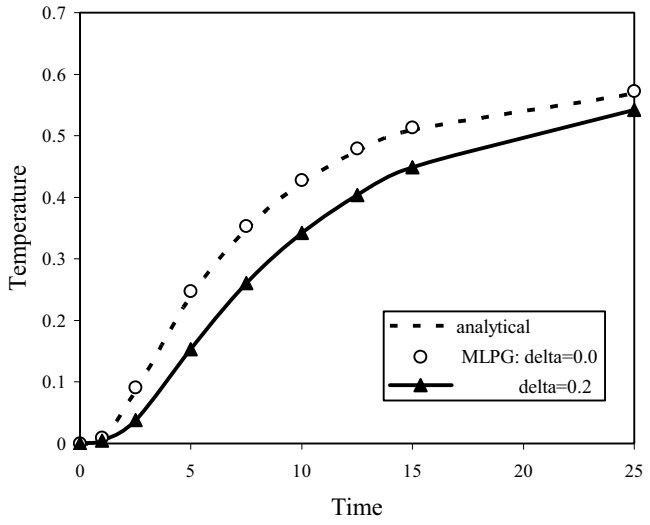

Figure 8 : Temporal variation of the temperature at the mid-radius $r = 12$

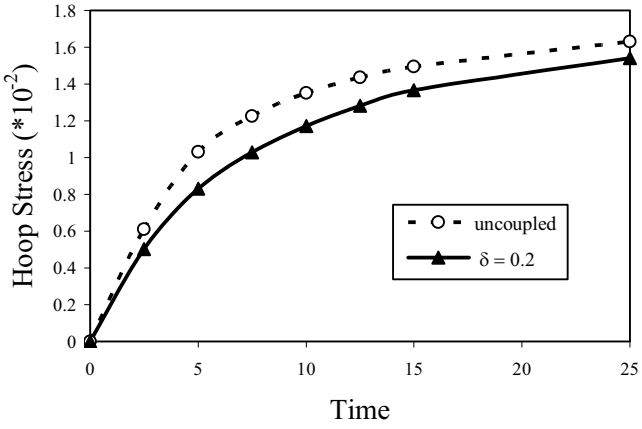

Figure 9 : Temporal variation of the hoop stress at the inner surface

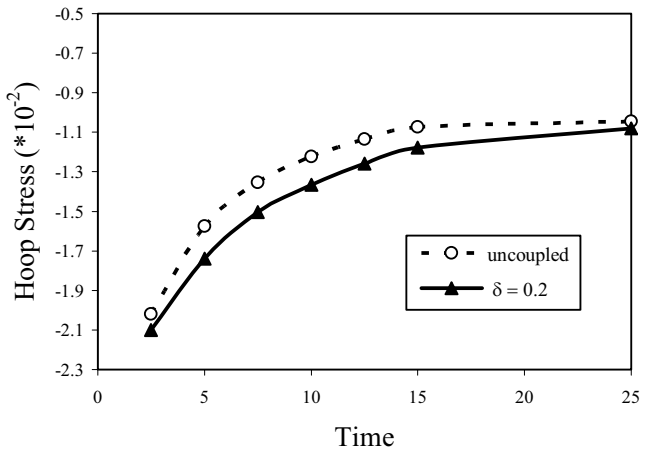

Figure 10 : Temporal variation of the hoop stress at the outer surface

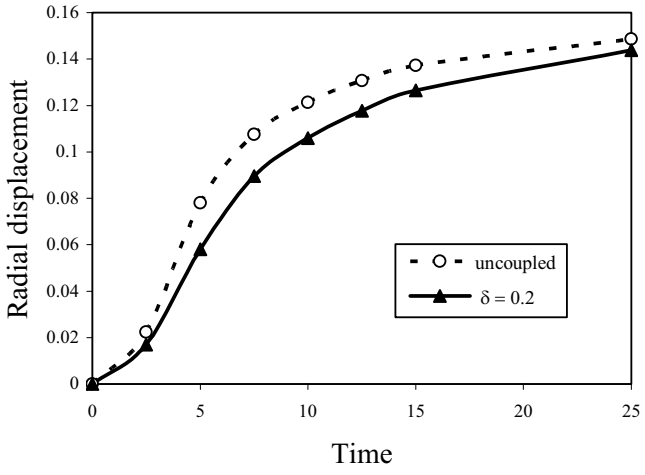

Figure 11 : Temporal variation of the radial displacement at the mid-radius

of the panel is considered here again. Isotropic material constants are assumed for the thermal coefficients and orthotropic for the mechanical ones. The following material constants are considered: $k = 1$, $\rho = 1$, $c = 1$, $\alpha = 0.02$, Young's modulii $E_1 = 1$, $E_2 = 2E_1$ and Poisson's ratio $\nu = 0.3$.

In uncoupled thermoelasticity, the same temporal variation of temperature as in the first example with results shown in Fig. 2 is obtained, since the thermal material parameters are the same in both cases. However, the displacements and the stresses are influenced by the mechanical material properties, which are the same as those used in the first example, except for the Young's modulus E_2. Numerical results for the displacement, u_2, at the free-end of the panel, $x_2 = 1$, and at the mid-side of the panel, $x_2 = 0.5$ are presented in Fig. 12. The displacements of the orthotropic panel are reduced in comparison with the isotropic one since the panel stiffness in $x_2$direction is larger than in the isotropic case. The direct stress σ_{11} at the mid side of the panel, $x_2 = 0.5$ is presented in Fig. 13. Here, σ_{11} is higher for the orthotropic panel than for the isotropic one. The influence of the coupling is investigated too. The temporal variations of the temperature computed in the framework of coupled thermoelasticity for isotropic and orthotropic panels are shown in Fig.14. One can observe that the influence of the orthotropic mechanical properties in the coupled theory has a negligibly small influence on the temperature

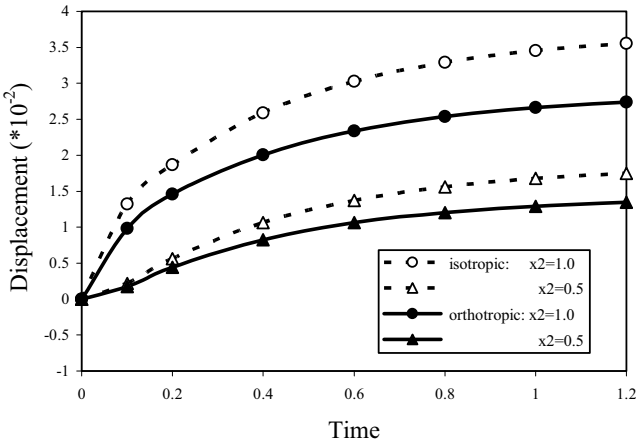

Figure 12 : Temporal variation of the displacement in uncoupled thermoelasticity for the orthotropic square panel

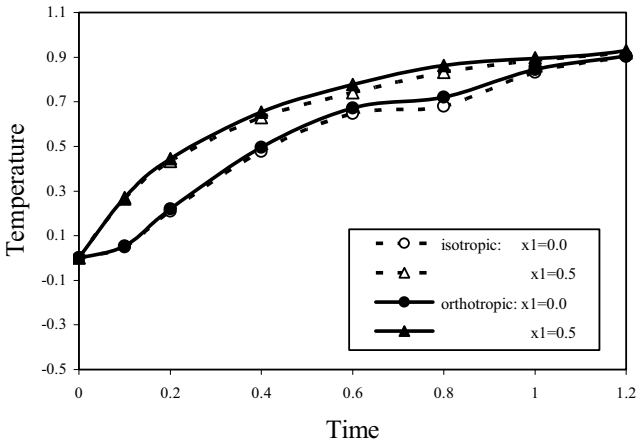

Figure 14 : Temporal variation of the temperature for coupled thermoelasticity

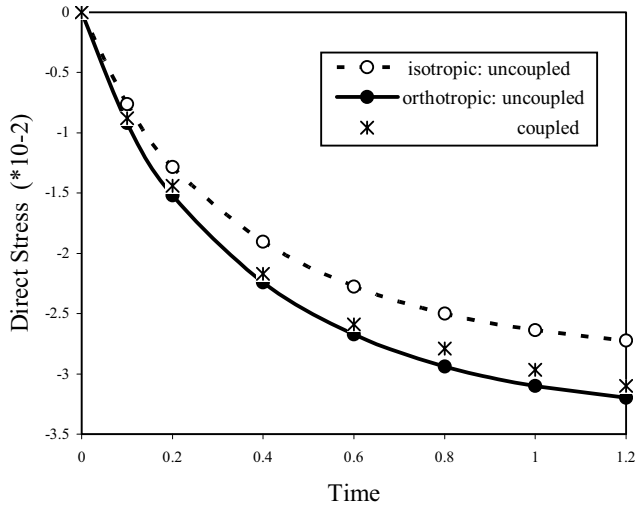

Figure 13 : Temporal variation of the direct stress σ_{11} in the orthotropic square panel

variation. A stronger influence of the orthotropic thermal properties on the temperature can be expected. On the other hand, the influence of the coupling on σ_{11}, as seen in Fig. 13, due to the orthotropy of the material is weak. The influence of the orthotropic mechanical properties on the mechanical stresses is much stronger than the mechanical-thermal coupling, at least in the cases considered here.

5 Conclusions

A meshless local Petrov-Galerkin method (MLPG) is presented for plane transient coupled thermoelasticity in orthotropic solids. The Laplace-transform technique is applied to eliminate the time variable in the coupled governing partial differential equations. The analyzed domain is divided into small overlapping circular subdomains. A unit step function is used as the test functions in the local weak-form. The derived local boundary-domain integral equations are nonsingular. The moving least-squares (MLS) scheme is adopted for approximating the physical quantities. The proposed method is a truly meshless method, which requires neither domain elements nor background cells in either the interpolation or the integration.

The present method is an alternative numerical tool to many existing computational methods such as FEM or conventional BEM. The main advantage of the present method is its simplicity in comparison with conventional BEM, where the fundamental solution is very complicated in the isotropic case, and for orthotropic materials it is even not available. In contrast to the conventional BEM, the present method requires no fundamental solutions and all integrands in the present formulation are regular. Thus, no special numerical techniques are required to evaluate the integrals. The present formulation possesses the generality of the FEM. Therefore, the method is promising for numerical analysis of multi-field problems, which cannot be solved effectively by the conventional BEM. Moreover, the present meshless method

seems to be more flexible than the standard FEM, since an adaptation of the nodal distribution is easier than a mesh adaptation.

The influence of the thermo-mechanical coupling on temperature and mechanical fields is investigated for both isotropic and orthotropic materials. In the present paper, only an orthotropy of the mechanical properties is considered in the numerical examples. The influence of the thermal orthotropy on both the mechanical and the thermal fields will be analyzed and reported in a future paper

Acknowledgement: The authors acknowledge the support by the Slovak Science and Technology Assistance Agency registered under number APVV-51-021205, the Slovak Grant Agency VEGA-2/6109/6, and the German Research Foundation (DFG) under the project number ZH 15/6-1.

References

Atluri, S.N. (2004): *The Meshless Method, (MLPG) For Domain & BIE Discretizations*, Tech Science Press.

Atluri, S.N.; Sladek, J.; Sladek, V.; Zhu, T. (2000): The local boundary integral equation (LBIE) and its meshless implementation for linear elasticity. *Comput. Mech.*, 25: 180-198.

Atluri, S.N.; Han, Z.D.; Shen, S. (2003): Meshless local Petrov-Galerkin (MLPG) approaches for solving the weakly-singular traction & displacement boundary integral equations. *CMES: Computer Modeling in Engineering & Sciences*, 4: 507-516.

Batra, R.C.; Porfiri, M.; Spinello, D. (2004): Treatment of material discontinuity in two Meshless local Petrov-Galerkin (MLPG) formulations of axisymmetric transient heat conduction. *Int. J. Num. Meth. Engn.*, 61: 2461-2479.

Belytschko, T.; Krogauz, Y.; Organ, D.; Fleming, M.; Krysl, P. (1996): Meshless methods; an overview and recent developments. *Comp. Meth. Appl. Mech. Engn.*, 139: 3-47.

Bobaru, F.; Mukherjee, S. (2003): Meshless approach to shape optimization of linear thermoelastic solids. *Int. J. Num. Meth. Engn.*, 53: 765-796.

Cannarozzi, A.A.; Ubertini, F. (2001): A mixed variational method for linear coupled thermoelastic analysis. *Int. J. Solids and Structures*, 38: 717-739.

Carslaw, H.S.; Jaeger, J.C. (1959): *Conduction of Heat in Solids*, Clarendon, Oxford.

Chen, J.; Dargush, G.F. (1995): Boundary element method for dynamic poroelastic and thermoelastic analyses. *Int. J. Solids and Structures*, 32: 2257-2278.

Dargush, G.F.; Banerjee, P.K. (1991): A new boundary element method for three-dimensional coupled problems of conduction and thermoelasticity. *ASME J. Appl. Mech.*, 58: 28-36.

Gaul, L.; Kögl, M.; Wagner, M. (2003): *Boundary Element Methods for Engineers and Scientists*. Springer-Verlag, Berlin.

Han, Z.D.; Atluri, S.N. (2004a): Meshless local Petrov-Galerkin (MLPG) approaches for solving 3D problems in elasto-statics. *CMES: Computer Modeling in Engineering & Sciences*, 6: 169-188.

Han, Z.D.; Atluri, S.N. (2004b): A meshless local Petrov-Galerkin (MLPG) approach for 3-dimensional elasto-dynamics. *CMC: Computers, Materials & Continua*, 1: 129-140.

Hosseini-Tehrani, P.; Eslami, M.R. (2000): BEM analysis of thermal and mechanical shock in a two-dimensional finite domain considering coupled thermoelasticity. *Engineering Analysis with Boundary Elements*, 24: 249-257.

Keramidas, G.A.; Ting, E.C. (1976): A finite element formulation for thermal stress analysis. I. Variational formulation, II. Finite element formulation. *Nuclear Engineering and Design*, 39: 267-287.

Kögl, M.; Gaul, L. (2000): *A dual reciprocity boundary element method for dynamic coupled anisotropic thermoelasticity*. In: Boundary Elements XXII, pp. 565-577, WIT Press, Southampton, UK.

Kögl, M.; Gaul, L. (2003): A boundary element method for anisotropic coupled thermoelasticity. *Arch. Appl. Mech.*, 73: 377-398.

Lekhnitskii, S.G. (1963): *Theory of Elasticity of an Anisotropic Body*, Holden Day, San Francisco.

Nowacki, W. (1986): *Thermoelasticity*, Pergamon, Oxford.

Park, K.H.; Banerjee, P.K. (2002): Two- and three-dimensional transient thermoelastic analysis by BEM via particular integrals. *Int. J. Solids and Structures*, 39: 2871-2892.

Prasad, N.N.V. (1998): *Thermomechanical Crack Growth using Boundary Elements*. WIT Press, Southampton, UK.

Prevost, J.H.; Tao, D. (1983): Finite element analysis of dynamic coupled thermoelasticity problems with relaxation times. *Journal of Applied Mechanics*, 50: 817-822.

Qian, L.F.; Batra, R.C. (2004): Transient thermoelastic deformations of thick functionally graded plate. *Jour. Thermal Stresses*, 27: 705-740.

Rizzo, F.J.; Shippy, D.J. (1977): An advanced boundary integral equation method for three-dimensional thermoelasticity. *Int. J. Num. Meth. Engn.*, 11: 1753-1768.

Sellountos, E.J.; Polyzos, D. (2003): A MLPG (LBIE) method for solving frequency domain elastic problems. *CMES: Computer Modeling in Engineering & Sciences*, 4: 619-636.

Sellountos, E.J.; Vavourakis, V.; Polyzos, D. (2005): A new singular/hypersingular MLPG (LBIE) method for 2D elastostatics. *CMES: Computer Modeling in Engineering & Sciences*, 7: 35-48.

Shiah, Y.C.; Tan, C.L. (1999): Exact boundary integral transformation of the thermoelastic domain integral in BEM for general 2D anisotropic elasticity. *Computational Mechanics*, 23: 87-96.

Sladek, V.; Sladek, J. (1984): Boundary integral equation method in thermoelasticity. Part I: General analysis. *Appl. Math. Modelling*, 7: 241-253.

Sladek, J.; Sladek, V.; Atluri, S.N. (2001): A pure contour formulation for meshless local boundary integral equation method in thermoelasticity. *CMES: Computer Modeling in Engineering & Sciences*, 2: 423-434.

Sladek, J.; Sladek, V.; Zhang, Ch. (2003a): Transient heat conduction analysis in functionally graded materials by the meshless local boundary integral equation method. *Computational Materials*, 28: 494-504.

Sladek, J.; Sladek, V.; Krivacek, J.; Zhang, Ch. (2003b): Local BIEM for transient heat conduction analysis in 3-D axisymmetric functionally graded solids. *Computational Mechanics*, 32: 169-176.

Sladek, J.; Sladek, V.; Atluri, S.N. (2004a): Meshless local Petrov-Galerkin method for heat conduction problem in an anisotropic medium. *CMES: Computer Modeling in Engineering & Sciences*, 6: 309-318.

Sladek, J.; Sladek, V.; Atluri, S.N. (2004b): Meshless local Petrov-Galerkin method in anisotropic elasticity. *CMES: Computer Modeling in Engineering & Sciences*, 6: 477-489.

Sladek, J.; Sladek, V.; Hellmich, Ch.; Eberhardsteiner, J. (2006): Heat conduction analysis of 3D axisymmetric and anisotropic FGM bodies by meshless local Petrov-Galerkin method. *Computational Mechanics* (in print).

Suh, I.G.; Tosaka, N. (1989): Application of the boundary element method to 3-D linear coupled thermoelasticity problems. *Theor. Appl. Mech.*, 38: 169-175.

Stehfest, H. (1970): Algorithm 368: numerical inversion of Laplace transform. *Comm. Assoc. Comput. Mach.*, 13: 47-49.

Timoshenko, S.P.; Goodier, J.N. (1951): *Theory of Elasticity*, McGraw-Hill, New York.

Wang, H.; Qin, Q.H.; Kang, Y.L. (2006): A meshless model for transient heat conduction in functionally graded materials. *Computational Mechanics*, 38: 51-60.

Zhu, T.; Zhang, J.D.; Atluri, S.N. (1998): A local boundary integral equation (LBIE) method in computational mechanics, and a meshless discretization approaches. *Computational Mechanics*, 21: 223-235.